NASA TECHNICAL NOTE

NASA TN D-2402

NASA TN D-2402

THE EFFECTS OF HIGH ALTITUDE EXPLOSIONS

by Wilmot N. Hess

Goddard Space Flight Center
Greenbelt, Md.

NATIONAL AERONAUTICS AND SPACE ADMINISTRATION • WASHINGTON, D. C. • SEPTEMBER 1964

THE EFFECTS OF HIGH ALTITUDE EXPLOSIONS

By Wilmot N. Hess

Goddard Space Flight Center
Greenbelt, Md.

NATIONAL AERONAUTICS AND SPACE ADMINISTRATION

For sale by the Office of Technical Services, Department of Commerce,
Washington, D.C. 20230 -- Price $1.00

THE EFFECTS OF HIGH ALTITUDE EXPLOSIONS

by
Wilmot N. Hess
Goddard Space Flight Center

SUMMARY

High altitude nuclear explosions have helped considerably in our understanding of the natural radiation belts. The Argus artificial radiation belt made in 1958 gave information on the stability of particle orbits. The Starfish artificial belt gave quantitative information on electron lifetimes not available any other place. Below L = 1.7 the electrons have a long life and apparently are lost only by coulomb scattering on the atmosphere. Above L = 1.7 the lifetime shortens abruptly and some non-atmospheric process dominates. Synchrotron radiation and aurora were also observed after Starfish. There are some interesting questions left about how the Starfish electrons got where they did and why they have the spectra observed.

CONTENTS

THE EFFECTS OF HIGH ALTITUDE EXPLOSIONS*

by
Wilmot N. Hess
Goddard Space Flight Center

INTRODUCTION

Seven artificial radiation belts have been made by the explosion of high altitude nuclear bombs since 1958. These artificial belts result from the release of energetic charged particles, mostly electrons, from the nuclear explosions. These seven explosions are:†

Explosion	Locale	Time	Yield	Altitude
Argus I	South Atlantic	1958	1 kt	300 miles
Argus II	South Atlantic	1958	1 kt	300 miles
Argus III	South Atlantic	1958	1 kt	300 miles
Starfish	Johnson Island, Pacific Ocean	July 9, 1962	1.4 Mt	400 km
USSR‡	Siberia	Oct. 22, 1962	Several hundred kt	?
USSR	Siberia	Oct. 28, 1962	?	?
USSR	Siberia	Nov. 1, 1962	?	?

The Argus explosions of 1958 were carried out to study the trapping of energetic particles by the earth's magnetic field. Nicholas Christofolis, a physicist at the Lawrence Radiation Laboratory, had for some time before Argus worked on Project Sherwood—the attempt to make controlled thermonuclear reactions in laboratory containers. To contain the intensely hot material used in the Sherwood experiments, no walls can be used; they would melt. Magnetic fields, shaped into "magnetic bottles" to contain the particles, are used. Such a bottle as that used in Figure 1 has been used successfully to contain hot electrons and protons for short times. The particles eventually leak out of the magnetic bottle, mostly through the ends, but they are contained for a time.

*To be published as a chapter in "Space Physics," edited by Donald P. LeGalley and Alan Rosen (publisher, John Wiley & Sons, Inc.).
†The U. S. explosions Teak and Orange in the Pacific (below 8 km) in 1958 may have injected some particles, but the effects here were small and short-lived. Another reported USSR high altitude explosion of 1961 may have produced some effects, but this is uncertain.
‡Atomic Energy Commission press releases of Oct. 22 and Nov. 1, 1962.

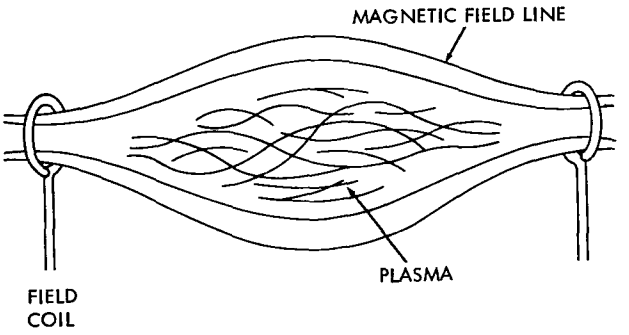

Figure 1—A magnetic bottle.

Christofilos took this idea for a laboratory-size magnetic bottle and expanded it to earth size. He suggested that the earth's magnetic field should be able to contain and trap energetic particles, and showed that a nuclear explosion would be a reasonable source of particles to populate the terrestrial bottle (Reference 1). This suggestion led to the Argus experiments.

The planning for Argus was well underway before the discovery by Van Allen of the natural radiation belt. In the Argus planning sessions it had been suggested that a natural belt might exist around the earth, which was of course borne out by the Explorer I (1958 $\alpha 1$) and Explorer III (1958 $\gamma 1$) satellites. After each of the Argus explosions, trapped particles were observed by Van Allen on the Explorer IV (1958 $\epsilon 1$) satellite (Reference 2).

The Starfish explosion of July 9, 1962, was of higher yield than Argus and made not only a more intense artificial belt but a considerably more extensive belt. This belt is of longer life than the Argus belts because it is at a lower latitude.

The three Soviet explosions of 1962 made artificial belts somewhat less intense than Starfish. These also were at high enough latitude so that they decayed rather rapidly. These three belts had different spatial extents, maybe indicating different altitudes for the explosions.

A BOMB AS A SOURCE OF CHARGED PARTICLES

What is there about a nuclear explosion that makes an artificial radiation belt? The radiation belts, both natural and artificial, are simply large populations of charged particles trapped by the earth's magnetic field to stay for long times near the earth. The natural belts are made up mostly of energetic electrons and protons plus small numbers of deuterons and tritons, and possibly some alpha particles and positrons as well. The artificial belts are made up mostly of electrons with some protons, and maybe some of the other particles too.

There are two kinds of nuclear explosions: fission, and fusion. The basic element of a fission reaction is the capture of a neutron by a heavy element, frequently U^{235}, which then fissions, or splits, into two lighter nuclei or fission fragments (Reference 3). In this process two or three neutrons are given off, of which about one per event may escape from the fissioning system. The neutron can produce trapped particles by decaying into a proton and an electron. At the time of fission, several gamma rays of roughly 1 Mev each are given off. These might produce some trapped electrons as the result of Compton scattering on air atoms, but the trapped flux of electrons produced by this process is probably small enough to be neglected. Some alpha particles are also given off by ternary fission. About 1 in 300 fissions produces an alpha particle of from 5 to

25 Mev. It is uncertain whether any of these alpha particles will get out of the fissioning system before they are slowed down to rest, but some of them may wind up trapped.*

After the fission process is over, more charged particles are given off. The fission fragments produced are unstable (they are neutron rich), and they decay by emitting electrons to become stable. One fission fragment emits about six electrons to become stable. These electrons are the most important source of all the artificial belts produced. They have energies up to about 8 Mev with an average energy of about 1 Mev. They can be released a long distance from the bomb because the fission fragment decay process is relatively slow. About one electron is given off in the first second after fission, and the other five are given off with a decay law.

$$N_e = N_e(0)\, t^{-1.2} ,$$

where t is in seconds. So electrons are still being given off minutes to hours after the explosion. If the fission fragments expand with a velocity of about 500 km/sec, electrons can be liberated up to 10^6 km away from the explosion site. But probably the expanding fission fragments are mostly ionized (Reference 4), and they will be trapped by the earth's magnetic field and cannot get nearly this far away from the explosion.

There also may be some positrons given off by radioactive debris after the explosion. One process that would cause this would be $(n, 2n)$ reactions; for example,

$$Al^{27}(n,\ 2n)\,Al^{26} .$$

The nucleus Al^{26} decays by positron emission. This probably is not a very important particle source.

A fusion bomb works by burning hydrogen to make helium. The end products are not radioactive, but some intermediate steps in the reaction produce charged particles that can be trapped. Deuterium and tritium are involved in the fusion process. Some tritons may be left after the reaction, but they probably are of quite low energy and are not interesting as far as radiation belts are concerned. Neutrons are produced by both (d, d) and (d, t) reactions. The neutrons from (d, d) reactions are of about 3 Mev, and those from (d, t) reactions are of 14 Mev. When these neutrons decay, they make electrons and also protons of 3 or 14 Mev, too; but, as we shall see, the yield of this reaction is quite small.

A fusion or hydrogen bomb explosion will produce a quite insignificant artificial radiation belt compared with fission or an atom bomb explosion of the same yield. The electrons from fission fragment β-decay are the most important source of particles for artificial radiation belts.

*Tilles, D., "On the Possibility of Alpha Particles in the Artificial Radiation Belt," submitted to *J. Geophys. Res.*

THE NEUTRON SOURCE

One of the sources of the artificial belts is neutrons given off by the explosion. We can evaluate the importance of this source.

About 10^{24} neutrons are given off by a 1-kiloton explosion. The neutrons are neutral and are therefore not trapped by the field, but they are radioactive and decay by the reaction $n \rightarrow e + p + \bar{\nu}$. The decay produces electrons and protons which can be trapped. The antineutrino $\bar{\nu}$ is of no interest to us here. The neutron mean life τ_n is 1000 seconds. The neutrons from fission are made with energies of about 1 Mev or a velocity v of about 10^9 cm/sec. They travel about 50,000 km to get out of the magnetosphere. A fraction of them will decay inside the magnetosphere, given by

$$f = \left(\frac{1}{1000}\right)\left(\frac{5 \times 10^9}{10^9}\right) = 0.005 .$$

Large enough charged particle fluxes will be made here to be important. The fraction of neutrons that decay will be larger for slower neutrons.

The electrons that are made by decay have energies up to 0.78 Mev with a peak in the spectrum at about 0.30 Mev. The electrons' energy is very nearly independent of the neutrons' energy. The decay protons, however, have energies nearly equal to the energy of the parent neutrons. This means that the protons from fission neutrons will be about 1 Mev. The proton flux from Starfish was probably about 10^4 protons/cm^2-sec of $E > 1$ Mev. Because the natural proton fluxes are considerably larger than this in most regions of space, we can ignore the neutron decay protons. The neutrons from the (d, t) reactions of the fusion bomb have 14 Mev protons; there will not be many of these. The 14 Mev neutron velocity is a factor of 4 larger than 1 Mev neutrons, so the fraction of them that decays is only 1/4 of the 1 Mev neutron decays. This means that for Starfish the 14 Mev proton flux will be less than 10^4/cm^2-sec.

However, the neutron decay electron flux is considerably higher than this (Reference 5). If M neutrons are given off by an explosion on the equator, the total neutron flux F at an observation point (see Figure 2) will be

$$F = \frac{M}{4\pi\rho^2} ,$$

where ρ is the distance from the explosion point to observation point; $\rho^2 = r^2 + R^2 - 2Rr \sin\theta \cos\varphi$. The neutron decay density from this flux will be

$$n_0 = \frac{M}{4\pi\rho^2 \, v\tau} \text{ decays/cm}^3 .$$

The explosion is a point source, but the particles will spread out in longitude by drift to form a shell. We can average the decay density in longitude

$$\bar{n}(r, \theta) = \frac{1}{\pi} \int_{-\phi_0}^{+\phi_0} n_0 (r, \theta, \phi)\, d\phi = \frac{M}{2\pi^2 v\tau} \int_0^{\phi_0} \frac{d\phi}{r^2 + R^2 - 2Rr \sin\theta \cos\phi} .$$

This space-averaged neutron decay density can be transformed directly to be an electron omnidirectional flux distribution in space.

If we have a neutron source above the atmosphere, we must consider not only neutrons traveling upwards away from the explosion but albedo neutrons from the top of the atmosphere. About 80 percent of the downward traveling neutrons will be reflected from the atmosphere and then travel upwards. In the reflection process the neutrons will be partly thermalized by collisions with air nuclei. As a result of this, the rate of decay of these neutrons will be higher and actually more total decays will result from the initially downward moving neutrons than from the upward moving ones. By carrying out these calculations and normalizing crudely to the Starfish explosion (Reference 5), we get the spatial distributions of electrons shown in Figure 3. The calculations have been made with and without albedo, and the importance of albedo in Figure 3 is obvious. Electron fluxes up to about 10^7 electrons/cm^2-sec

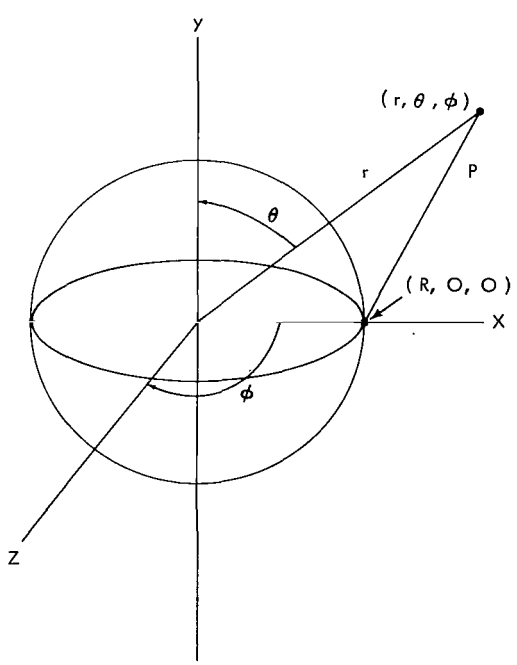

Figure 2—The geometry of the point source of neutrons.

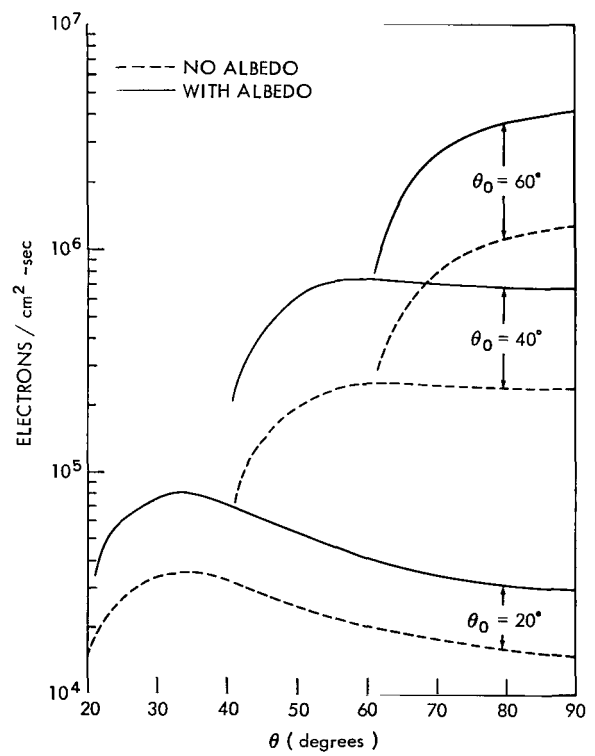

Figure 3—The calculated initial electron fluxes from neutron decay from Starfish, with and without albedo from the top of the atmosphere (from Reference 5). Different field lines are identified by their earth surface colatitudes θ_0.

are expected from neutron decay from Starfish. These are initial fluxes and will, of course, decay with time. This flux is not negligible, but it is concealed by the considerably larger flux of fission electrons.

PARTICLE MOTION

We need to understand the motion of charged particles in a magnetic field in order to understand how an artificial belt of particles surrounding the earth is made from a point source explosion. For the particles of interest to us, we can break this motion down into three components (see Figure 4):

(1) A rapid gyration of the particles around the field line,
(2) A bouncing back and forth along a field line from one hemisphere to the other, and
(3) A slow drift in longitude around the earth.

The gyration period or cyclotron period of an electron in the earth's field is roughly a microsecond. The bounce period is of the order of 1 second.

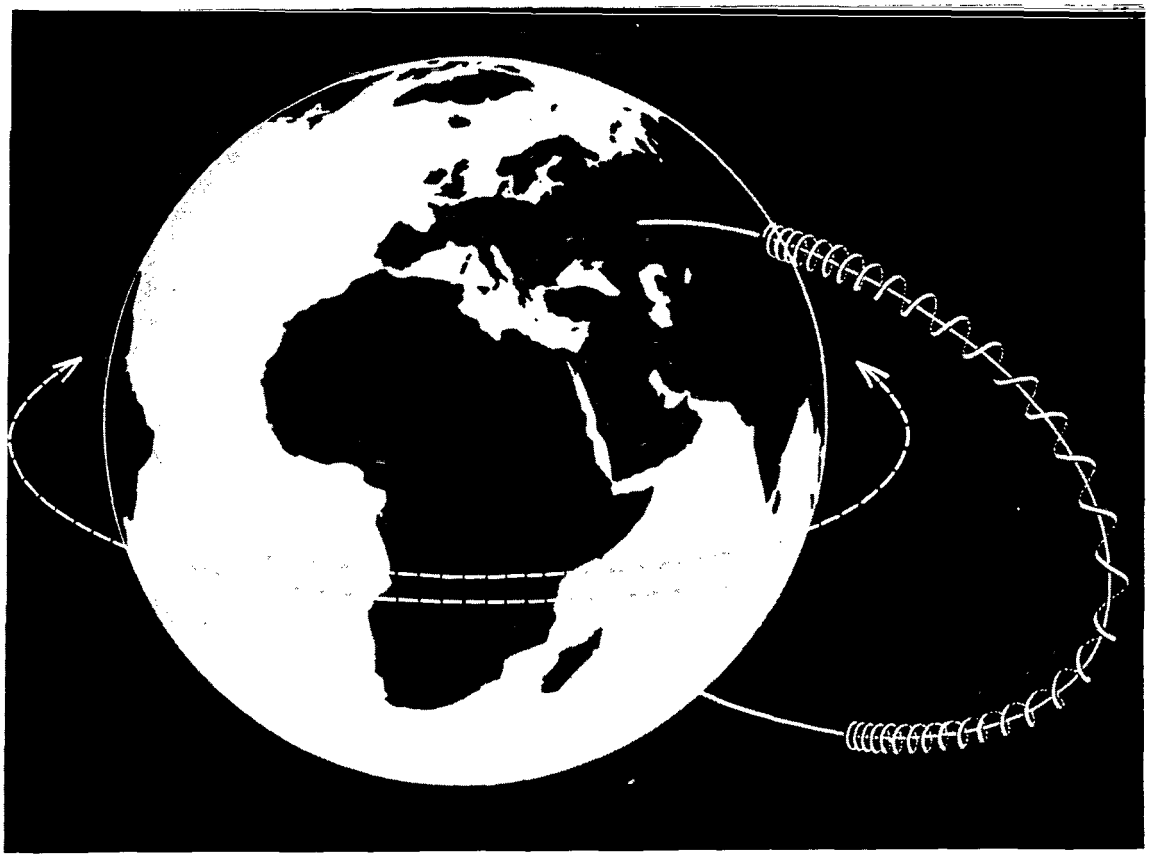

Figure 4—Motion of charged particles in a dipole magnetic field.

It is essential to understand the phenomena of bouncing to see how a radiation belt can exist. Whenever a gyrating charged particle moves into a converging magnetic field, there is a force produced that tends to push the particle out of the converging region. This force is

$$F = v \times B \approx V_\theta B_r ,$$

where V_θ is the component of the particle's velocity around the field line and B_r is the component of the magnetic field perpendicular to the axis of symmetry ($B_r = 0$ for a uniform field). The force F is always directed out of the region of convergence. Near each end of one of the earth's field lines, the field converges towards the surface of the earth; therefore, the force F acts like a restoring force which tends to push the particle along the field line towards the equator. As a result, a bouncing motion much like the oscillation of a pendulum takes place. This bouncing motion takes place with a magnetic moment μ of the particle a constant of the motion. The magnetic moment is defined by

$$\mu = \frac{E_\perp}{B} = \frac{\frac{1}{2} m V_\perp^2}{B} = \frac{\frac{1}{2} m V^2 \sin^2 \alpha}{B} ,$$

where $E_\perp$ is the particle's kinetic energy associated with the gyration and α is the angle between V and B called the pitch angle. A static magnetic field does no work on a particle so V = constant; and, because μ is a constant,

$$\frac{\sin^2 \alpha}{B} = \text{Constant} .$$

During the bouncing motion, α changes as B does, according to this equation. The particle turns around when $\sin \alpha = 1$ or at a magnetic field strength B_m, given by

$$\frac{\sin^2 \alpha}{B} = \frac{1}{B_m} .$$

This point of field B_m is called the particle's mirror point. A particle's mirror point depends only on its initial pitch angle α (not on its energy). If the value of B_m for a particle is below ground level or in the dense atmosphere, this particle will be lost right away.

The particles also drift in longitude around the earth. There are two effects that produce this drift. The radial gradient of the magnetic field and the curvature of the field lines both act to make the electrons drift east and the protons west. The field gradient effect can be understood by considering the gyration of the particle around the field line. Because of the field gradient, the cyclotron radius is larger on the high altitude side of the line. This asymmetry in the gyration causes the particle to move sideways as shown in Figure 5. Particles with higher velocity drift faster in longitude. A fission electron takes about 1/2 hour to drift around the earth. As the particle drifts in longitude, it moves from one field line to another. Which new field line the particle moves to is

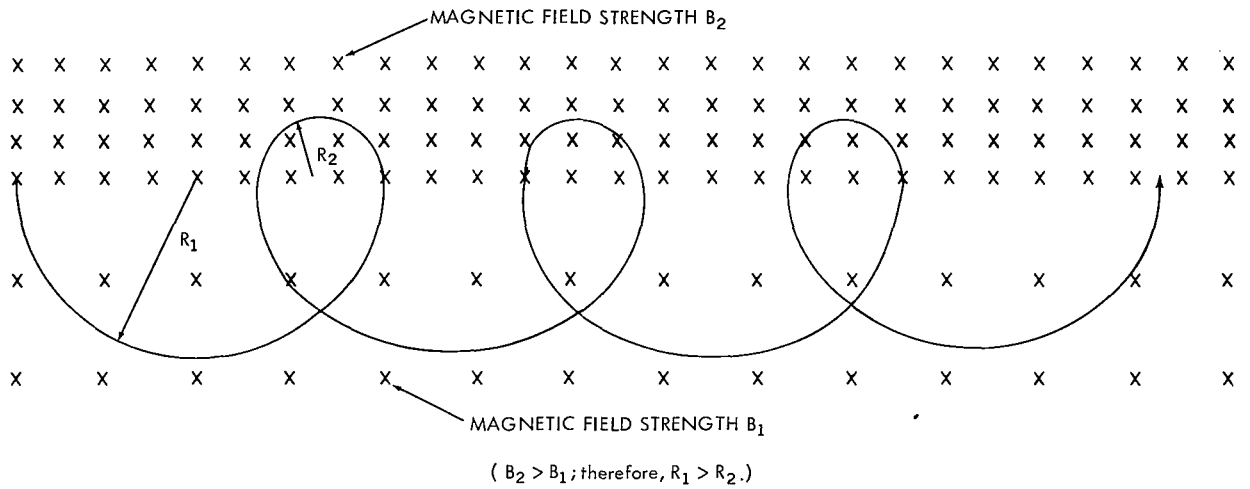

Figure 5—Drift of a charged particle in a magnetic field with a gradient.

determined by the fact that

$$I = \int \cos \alpha \, d\ell = \int_{B_m}^{B_m^*} \sqrt{1 - B/B_m} \, d\ell$$

is a constant of the motion (where the integral is taken along a field line from one mirror point B_m to the other B_m^*). Actually, I is only an adiabatic constant of the motion. If B changes in a time short compared with the bounce time, then I is not a constant. The magnetic moment μ is also only an adiabatic constant of the motion.

The integral invariant I is a kind of weighted length of the field line between B_m and B_m^*. As the particle drifts from one field line to a new one, the value of B_m at the mirror point stays constant because μ is a constant of the motion. Also, I remains constant during the drift, so the length of the field line from B_m to B_m^* remains constant. As the particle drifts in longitude around the earth, only one set of field lines will satisfy these constraints and the particle will return to the line it started on. McIlwain has introduced a parameter L to label such a shell of field lines. In a dipole field, L would be the distance from the center of the earth to the equatorial crossing of the field line in units of earth radii. The shell $L = 2$ would go to 6370 km altitude at the equator. For the real field of the earth, which varies considerably from a dipole, the definition of L is more complicated. However, the $L = 2$ shell still has an average equatorial altitude of about 6370 km, although it varies about ±500 km from this.

We now can understand what happens to particles emitted at one point in space by a nuclear explosion. In a few seconds they are spread out along a field line, and in a few hours they drift around the earth and spread out in longitude to form a blanket around the earth. The thickness of the blanket depends on the initial dimensions of the particle source.

EARLY HISTORY OF STARFISH

We now have an idea about what should happen to the particles from an explosion. Let us see what the observations show after the Starfish explosion of July 9.

Magnetic and electromagnetic signals and a whistler radiated by the explosion were observed at several places (References 6, 7, 8, and 9). These may play a part in the artificial belt; they may interact with particles in the natural belt, and either change their energy or scatter them and change their pitch angle. These changes in the naturally trapped particles may produce some of the observed effects.

Just seconds after the explosion, artificial auroras were observed in New Zealand (Reference 10). These are produced by the electrons and other particles from the explosion that are not trapped. Because lots of these particles have mirror points below the atmosphere, they will enter the atmosphere and interact with oxygen and nitrogen atoms. The excited atoms will emit light to form the aurora. Rockets have been flown into natural aurora and energetic electrons found, so this process of electrons making auroras is well established.

Just 2 seconds after the explosion, increased ionospheric absorption of cosmic radio noise was observed in Alaska (Reference 11) at $L \approx 6$. This is probably due to debris from the explosion traveling upwards to these field lines and releasing electrons β-decay, some of which promptly are lost into the atmosphere. The increased ionospheric electron densities produced this way would enhance the cosmic noise absorption. The peak absorption was detected within 1 minute after the explosion, followed by recovery to normal in a few hours. Attenuation like this was not observed in the U. S. at the same distance as Alaska or in the auroral region in Canada or Norway, so the effect is clearly associated with early time effects of charged particles from the explosion.

A few minutes after the explosion increased, f_{min} was observed on an ionosonde in Jamaica (Reference 12), indicating increased absorption in the lower regions of the ionosphere. This must have been due to trapped electrons drifting east and some of them getting lost as they went.

Topside soundings of the ionosphere on Ariel I, 1962 o1 (Reference 13) also showed increased electron densities in the ionosphere above the F_2 layer shortly after the explosion.

There also will be increased electron densities in the region near the explosion because of absorption of soft x rays from the explosion (as much as half the energy of the explosion may be in the form of these soft x rays) (Reference 14). But this effect will only be line of sight from the explosion and cannot explain the Alaska or Jamaica observations.

SYNCHROTRON RADIATION

A few minutes after Starfish, synchrotron radiation from the trapped electron was observed in Peru (Reference 15). This is the only effect of the artificial radiation belts that is observed on the ground for long periods. Synchrotron radiation is the electromagnetic radiation given off when an

electric charge is accelerated in a circle (Reference 16). It was first observed as light emitted from a synchrotron electron accelerator. If the charged particles have $V << c$, then the radiation is emitted only at the cyclotron frequency and is called *cyclotron radiation*; but, when the particle is relativistic, many higher harmonics of the cyclotron frequency are emitted, too, and the radiation is called *synchrotron radiation*. The radio emission of the planet Jupiter in the 30 cm range is tentatively identified as being synchrotron radiation from trapped electrons with energies in the order of 5 to 100 Mev (Reference 17).

The total power radiated by a particle by synchrotron radiation is

$$P = \frac{2}{3} \frac{e^2}{c^3} \left(\frac{dV}{dt}\right)^2 .$$

An expression that is more useful in comparison with experiments is the power spectrum radiated in the electrons' orbited plane for a relativistic electron (Reference 18):

$$P(f) = 4.1 \times 10^{-30} B\gamma F(f) \text{ watts/cps-ster} ,$$

where B is the magnetic field strength in grams, γ is the relativistic energy factor E/m_0c^2, and $F(f)$ is a function of the frequency f. Evaluating $P(f)$ at 50 Mc for $B = 0.16$ gauss and $E = 2$ Mev gives $P(f) = 4 \times 10^{-3}$ watts/cps-ster. Integrating $P(f)$ over the electron spatial distribution and fission energy spectrum for Starfish and integrating over antenna patterns gave calculated sky brightnesses in very good agreement with those measured shortly after Starfish (Reference 19).

Attempts were made to observe synchrotron radiation from the natural Van Allen belt before Starfish, but it could not be measured because of the background of other natural radio noises. After the Starfish explosion, synchrotron radiation was observed by several stations. The Bureau of Standards has a radio observatory in Peru which contains about 20,000 dipoles (Reference 15); this array can study the radio noise coming in a narrow angle from the zenith (which is very nearly the magnetic equator). The newly trapped electrons from Starfish produced more synchrotron noise than the natural belt electrons because there were more of them and they were of higher energy. The maximum 50 Mc signal at Peru arrived at +6 minutes after the explosion. This delay time is compatible with the time required for a 2.7 Mev electron to drift in longitude from the location of the explosion to Peru. A second peak was seen about 35 minutes later because of the electrons drifting around the world a second time. After this, the noise was nearly constant because the electrons had dispersed in longitude because of their different velocities. Polarization measurements made at Peru with the dipole array show the radio noise received was roughly east-west linearly polarized, as is expected for synchrotron radiation.

Several other antennas measured the synchrotron radiation after Starfish (Reference 20). At Wake Island the maximum signal was obtained at +25 minutes. This later arrival than at Peru shows that electrons drift east as expected. This delay time is right for about 2 Mev electrons.

Comparing several receiving stations shows that only stations within 25 degrees of the magnetic equator detected synchrotron radiation. This is reasonable because the radiation is given off in the instantaneous direction of motion of the electron, and this means that large signals should be found at the equator and the signal should decrease rapidly going off the equator.

Observations at Peru showed that the synchrotron noise decayed with a time behavior given by

$$n = n_0 \frac{1}{1 + \left(\frac{t}{60}\right)} ,$$

where t is the time in days after Starfish. This time decay is not representative of the decay of the artificial radiation belt as a whole because a large fraction of the synchrotron noise is given off by low altitude electrons where the magnetic field B is large. These low altitude electrons will be lost quite rapidly.

SATELLITE DATA ON STARFISH

On July 10 there were in orbit four satellites that had electron detectors on board and gave useful information on the newly trapped particles.

Satellite	Apogee (km)	Perigee (km)	Inclination (degrees)	Detectors
Ariel I	1209	393	54	Shielded GM counter, $E_e > 4.7$ Mev
Injun (1961 o 1)	1010	890	67	Shielded GM counter, counting several Mev electrons by bremsstrahlung
Telstar I (1962 A-ϵ1)	5630	955	44.7	4-channel solid state detector, $E_e > 0.2$ Mev
Traac (1961 A-η2)	1110	951	32.4	Shielded GM counter, $E_e > 1.6$ Mev

The Injun satellite had been in orbit a long time, and so it provided a very good "before-after" comparison of the radiation belt. The Traac detector also showed a good comparison this way, as did Ariel I. Unfortunately, Telstar I was launched the day *after* Starfish, so it could not give a before-after comparison. This is quite unfortunate, because the Telstar satellite goes to high altitudes and maps out regions of space that are unavailable to the other satellites.

The joint U. S.-U. K. satellite Ariel I showed that high energy electrons resulting from the bomb appeared very shortly after the explosion at high latitudes—up to $L = 5$ or more (Reference 21). Ariel I went out of operation a week after Starfish, but during this time the flux of energetic electrons stayed high up to $L = 5$.

The Traac detectors followed the decay of low altitude Starfish electrons until it also went out of operation (Reference 22). Traac located a puddle of fission debris sitting on top of the atmosphere in the Pacific, continuously emitting electrons into the belt (Reference 23). These new electrons from the debris puddle will have short lives, because they are emitted at low altitudes and therefore have low mirror points and encounter a fairly dense atmosphere.

By comparing the measurements of the several different detectors having different energy responses, the energy spectrum of the new particles was determined. At about 1000 km the spectrum closely resembled a fission energy spectrum, thus identifying the decay of fission fragments as the major particle source (Reference 24).

The Injun counters mapped out the new belt at 1000 km altitude and produced the first flux contour picture of the Starfish electrons (Reference 25). The Telstar satellite produced all of the information above 1000 km for the first three months after Starfish (Reference 26). The experimental data from Injun and Telstar for a short period after Starfish were organized and plotted. A comparison of these data is shown in Figure 6. The region of highest flux for the Injun data is

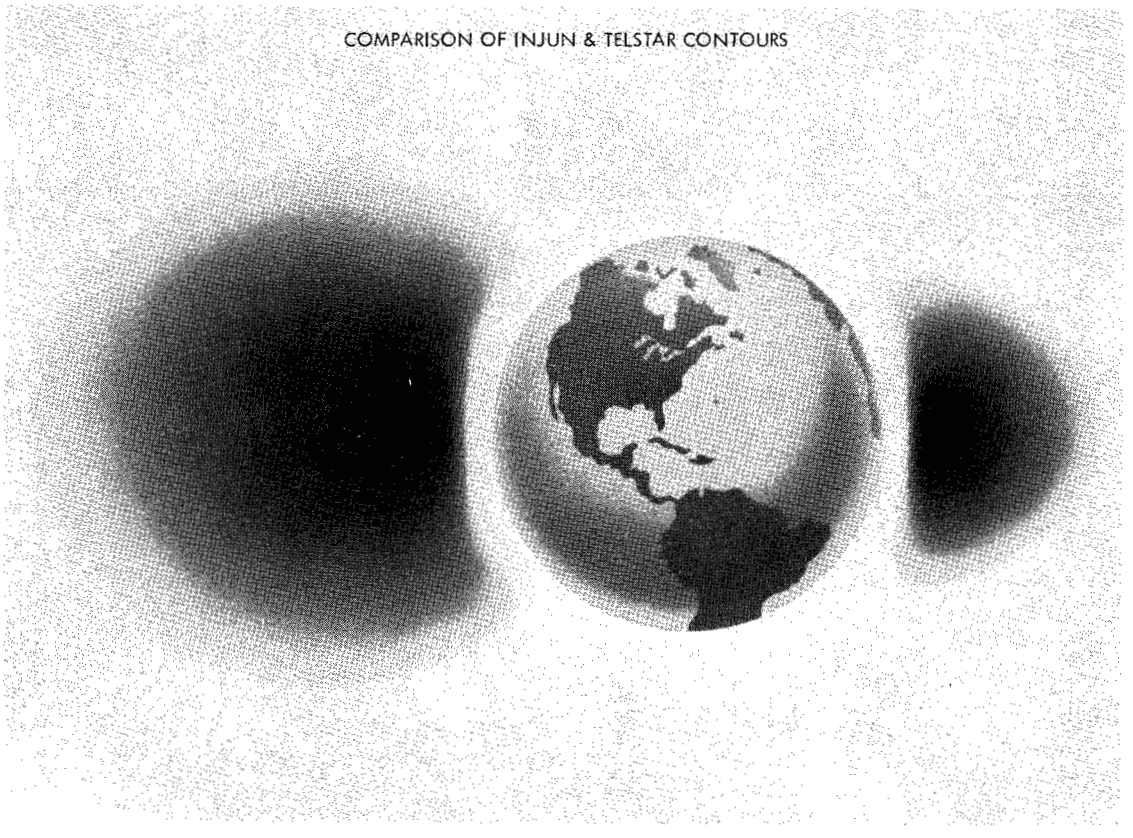

Figure 6—A comparison of the electron flux distribution measured by Telstar I (on the left) and Injun (on the right) shortly after Starfish. Both distributions are arbitrarily cut off at the outside at a flux of 10^7 electrons/cm^2-sec.

about 10^9 electrons/cm^2-sec, and for the Telstar data the highest value is also about 10^9 electrons/cm^2-sec. The outer edge of both flux distributions shown is at a flux of 10^7 electrons/cm^2-sec. These distributions in Figure 6 are only approximate and involve some extrapolations in both cases.* Also they are not for the same time (Injun is +10 hours and Telstar is +5 days), but they still are fairly accurate and can be compared reasonably. It is obvious the Injun flux distribution is much more compressed than is Telstar's. The total number of particles found by integrating inside the Injun distribution is about 10^{25} electrons (Reference 28) and inside the Telstar picture is about 10^{26} electrons (Reference 26). This difference is reasonably well understood now. We will return to this point later.

A map of the Starfish electron fluxes at 400 km altitude above the earth is shown in Figure 7. These are the fluxes as of one week after Starfish. They have decayed probably about a factor of 10 up to the present. The reason why large fluxes are seen in the South Atlantic and not elsewhere has to do with the earth's magnetic field. Since the field is weakest here, electrons—in order to satisfy the condition of mirroring at a certain value of B_m—must come closest to the earth in this region. Therefore the largest flux is seen in this region.

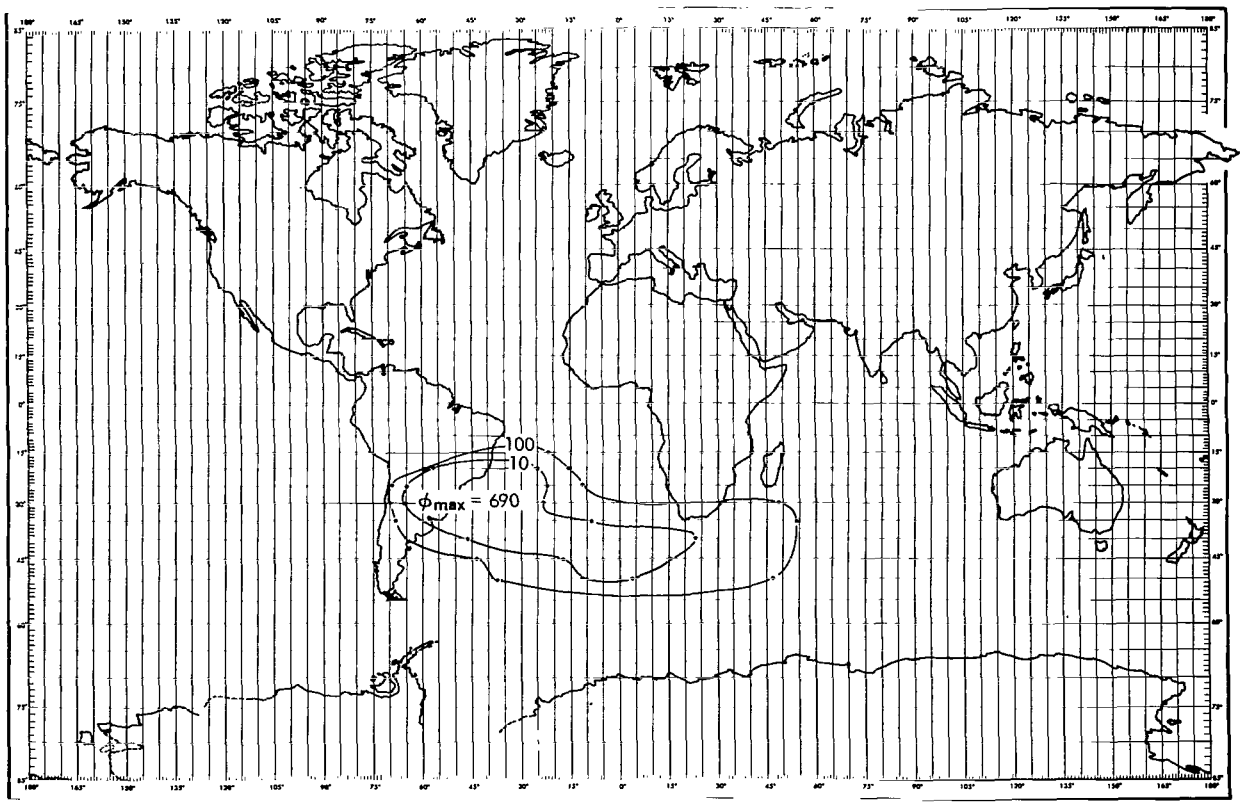

Figure 7—A map of electron fluxes at 400 kilometers altitude shortly after Starfish.

*The best Telstar contours are given in Reference 27, and the best Injun data in References 25 and 28.

The spatial distribution of electrons from Starfish is not easy to understand. The ionized debris from an explosion will expand outwards and, because the debris will be a good conductor, it will push the magnetic field ahead of it. In this way a bubble will be blown in the magnetic field (Reference 29). The bubble will stop expanding when the energy in the excluded field equals the initial kinetic energy E of the debris:

$$E = \frac{B^2}{8\pi} V = \left(\frac{B^2}{8\pi}\right)\left(\frac{4\pi R^3}{3}\right) = \frac{B^2 R^3}{6} .$$

The bubble will collapse and leave behind a region about the size of the bubble filled with fission fragments and electrons. For the Argus explosion, $E \approx 1$ kt $= 4 \times 10^{19}$ ergs. For $B = 0.3$ gauss we get $R \approx 100$ km. This is the approximate measured thickness of the Argus electron shells (Reference 2).

However, this simple model does not work for Starfish. The radius here would be $R \approx 1000$ km, but actually the debris must have gone considerably farther than this. To get to $L = 5$, the bubble would have to be about twice this diameter if it grows across field lines or even larger if it grows upwards. The bubble might break up into several bubblets to allow the electrons to disperse more.

Several satellites launched after Starfish have made measurements on the artificial belts and have confirmed the general picture of the electron flux distribution. A magnetic spectrometer flown on the Air Force satellite 1962 βK measured the electron energy spectra from Starfish at different L values (Reference 30). Such spectra for December 8, 1962, are shown in Figure 8. At $L = 1.25$ the energy spectrum looks like the fission spectrum (curve A, Figure 8) except that there are fewer low energy electrons. These low energy electrons probably have been lost by coulomb scattering between July and December. The measured spectrum at $L = 1.57$ is softer. It has considerably fewer high energy electrons than a fission spectrum. Not much decay has taken place here, so this spectrum should be quite like the initial spectrum on July 9 at $L = 1.57$.

This information on the energy spectrum helps in understanding the difference in the Telstar I and Injun flux distributions in Figure 6. In developing these flux distributions, it was assumed that all the electrons involved had a fission energy spectrum. The Injun detector does not count electrons of $E < 2$ Mev efficiently. The Telstar detector does count low energy electrons with $E < 1$ Mev well. This means that Telstar will count the soft electrons at $L = 1.57$ much more efficiently than will Injun. Because of this, the Injun contours should close at lower altitude than the Telstar contours. These two sets of contours are two different pictures of the same thing. The Injun picture shows the spatial distribution of electrons of $E \approx 3$ Mev. The Telstar picture shows the spatial distribution of $E \approx 1/2$ Mev electrons, and probably gives a better estimate of the total artificial belt electron population than the Injun estimate because Injun does not include the large number of low energy electrons present.

Several satellites have followed the decay of the Starfish electrons. This will be considered in a later section.

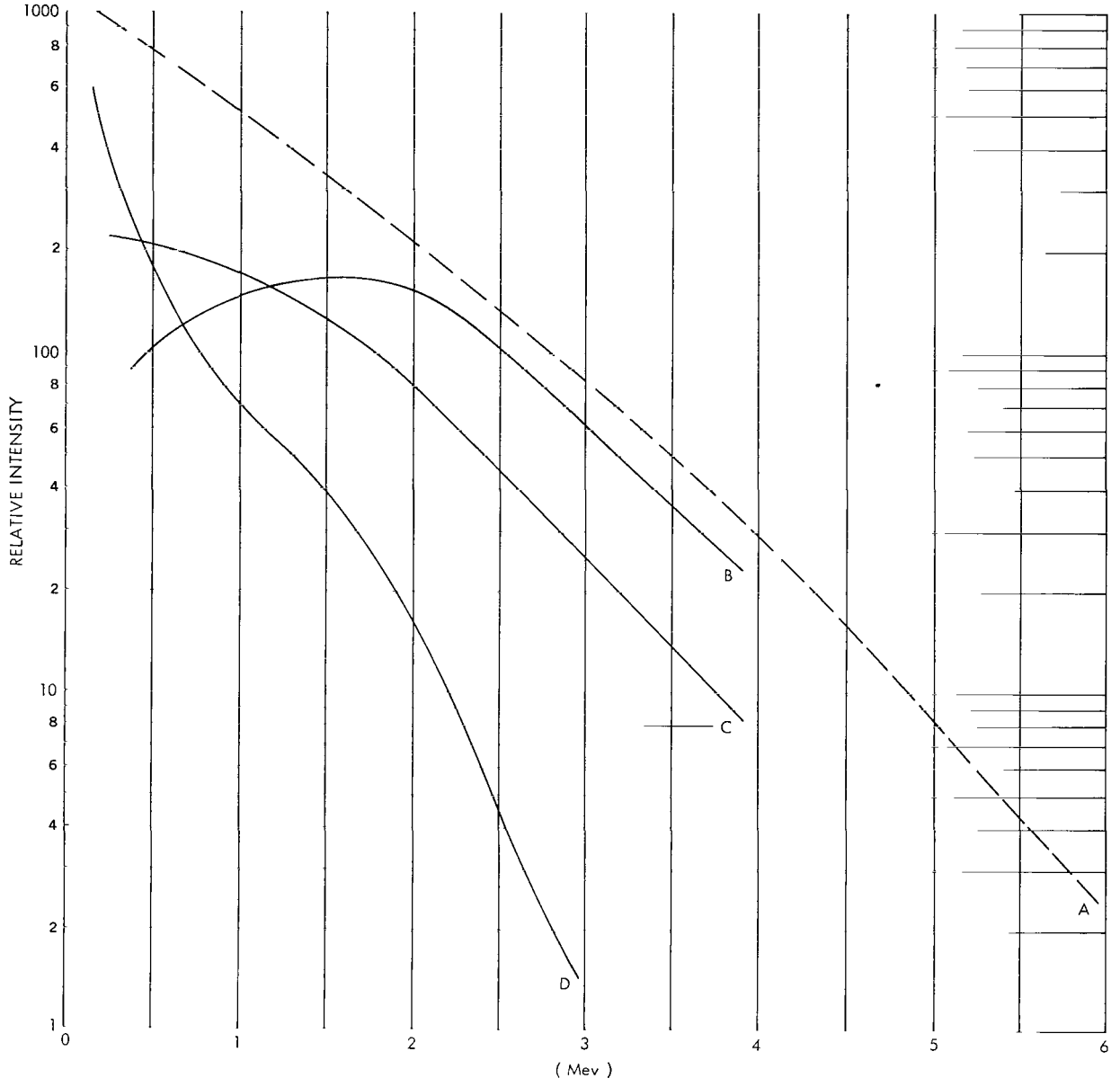

Figure 8—Various electron energy spectra: (A) the equilibrium fission energy spectrum; (B) the spectrum measured at L = 1.25 on Dec. 8, 1962; (C) the spectrum measured at L = 1.34 on Dec. 8, 1962; (D) the spectrum measured at L = 1.57 on Dec. 8, 1962 (from Reference 31).

RADIATION DAMAGE

The artificial radiation belt can cause damage to radiation-sensitive components such as solar cells—and man. The same, of course, is true of the natural radiation belt. The power supplies of three satellites were damaged by the Starfish electrons. The Ariel I satellite went into intermittent operation after about 1 week, and the Traac and Transit 4B satellites stopped in about 1 month. The

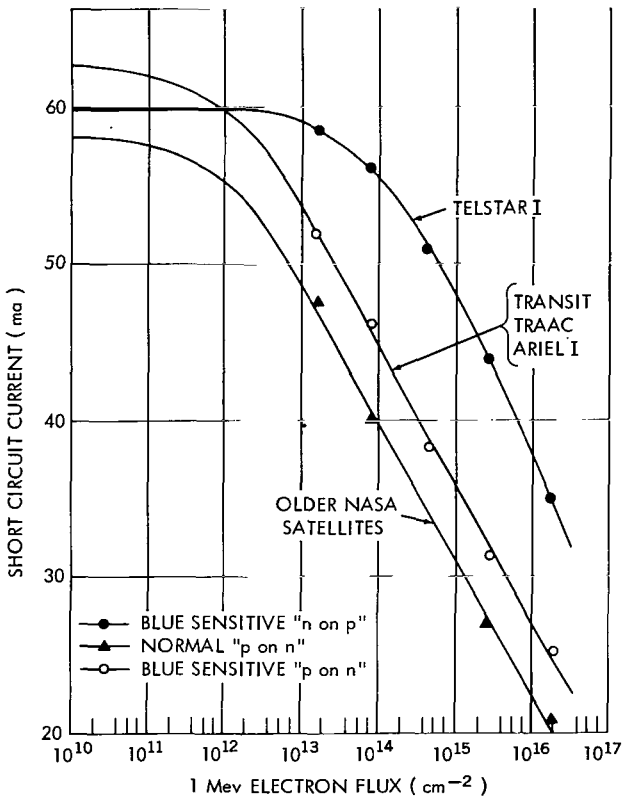

Figure 9–Solar cell degradation due to 1 Mev electron bombardment (from Reference 33).

solar cells on these satellites were progressively deteriorated because of the artificial electrons from Starfish. The output current of a solar cell goes down as the radiation exposure goes up (Reference 32), as shown in Figure 9. A normally designed satellite power supply will malfunction if the solar cell output drops to about 80 percent of its designed value. Figure 9 shows that this will take about 10^{13} electrons/cm^2 for the p-on-n type solar cells used on Ariel. Ariel I stays in the high flux region of 10^9 electrons/cm^2-sec about 10 percent of the time, so it encounters roughly 10^{12} electrons/cm^2-day; and a week is about the right time for the power supply to last before going into undervoltage. The output from the solar cells on Traac and Transit 4B was monitored (Reference 34), and the time history is shown in Figure 10. The initial slow decrease is due to the natural trapped particles, and the sudden change on July 9 is clearly due to the trapped electrons from Starfish. Telstar I, with a different and more radiation-resistant n-on-p type solar cell, lived a long time in the artificial radiation belt. Injun also lasted a long time after Starfish because its power supply was built to stand a larger percentage degradation and therefore more radiation. Satellites clearly can be designed to have long lives in the Starfish belt, or even more intense belts; but Ariel I, Traac, and Transit 4B were not expected to encounter these radiation levels, and so they were not designed for it.

A total flux of 3×10^7 particles/cm^2 is equivalent to 1 Rad (if the charged particles are minimum ionizing). The flux of natural high energy protons is about 2×10^4/cm^2-sec. This will result in about a 10 Rad/hour radiation dose to a lightly shielded person. The high electron flux region from Starfish has about 10^9 electrons/cm^2-sec. This would result in about 30 Rad/sec. Shielding can be used to reduce the radiation dosage. For a fission energy spectrum, 1 gm/cm^2 of shielding material will reduce the dose about a factor of 10, 2 gm/cm^2 a factor of 100, and 3 gm/cm^2 a factor of 1000. But it is quite difficult to reduce the radiation by more than a factor of 5000 because of the x rays produced by the electrons hitting the shielding. The fraction f of the electrons' energy that goes into bremsstrahlung is about

$$f = \frac{ZE^2}{1600} .$$

For fission electrons incident on an aluminum shield, $f \approx 0.01$. The absorption length of the

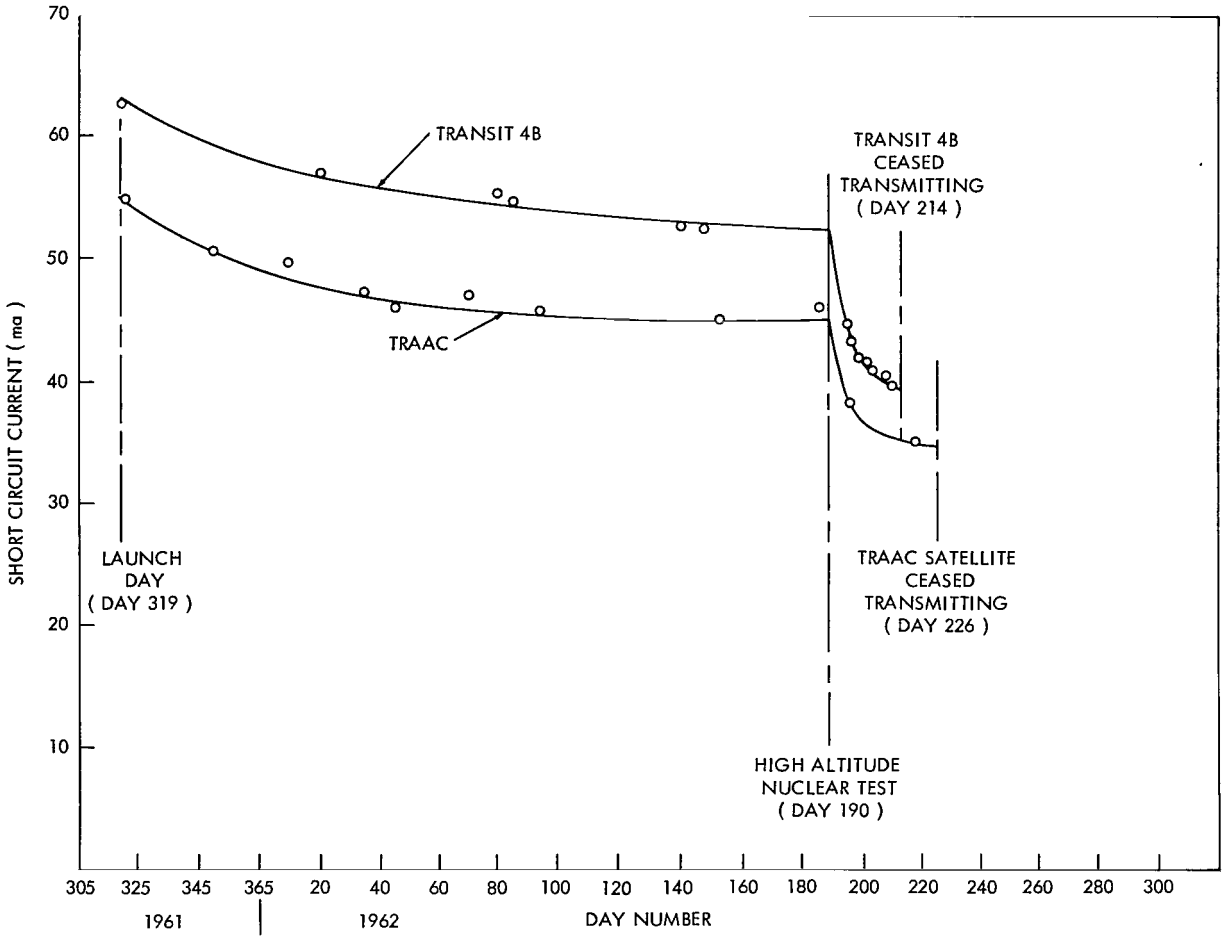

Figure 10—The time history of the solar cell output from Traac and Transit 4B (from Reference 35).

bremsstrahlung x rays is about 20 gm/cm^2, so the rate of energy loss is about a factor of 50 less than for minimum ionizing charged particles. Combining these factors gives a reduction of a factor of 5000 in the rate of energy deposition under the shield. But the x rays that are produced, having an absorption length of 20 gm/cm^2, are very hard to absorb out; so additional shielding after about 4 gm/cm^2 does not help much.

With a factor of 5000 reduction in radiation due to shielding, the radiation dose from the Starfish flux would still reach about 20 Rad/hr. Since about 500 Rad is lethal to most people, this region of space cannot be used for prolonged manned space flight.

Attention was given to the problem of manned flight shortly after Starfish. The flux map for 1 week after Starfish was used to calculate that about 1 Rad radiation dose would be received by an astronaut on a six-orbit mission at that time (Reference 24). By the time the MA-8 flight took place, decay of the trapped particles had reduced the expected dose considerably, and the dose received was well under 1 Rad. This is less than is received in some chest x rays and is not a problem.

EFFECTS ON THE NATURAL RADIATION BELT

The question had been raised before Starfish as to whether the explosion would seriously alter the natural Van Allen belt. Most opinion was that it would not. Because of the large flux of artificial electrons injected by Starfish, it is not possible to say anything about changes to the natural belt electrons. However, there is some information about the high energy proton fluxes. Nuclear emulsions flown on recoverable satellites measured the 55 Mev proton flux at various times before and after Starfish.* About 3 weeks after Starfish the 55 Mev proton flux at 400 km was about a factor of 5 larger than before Starfish. It has decayed since then. There is some uncertainty about the rate of decay of the protons, but the decay constant is of the order of 10^7 seconds. There is no source of 55 Mev protons from the explosion, so these particles must be natural belt protons. Very likely the explosion displaced a small fraction of the high energy Van Allen belt protons. The hydromagnetic wave from the explosion might do it, but the details of such a process are not understood quantitatively.

If only a few percent of the high energy protons at high altitudes were moved downwards, this observation could be explained. The high energy proton flux at high altitudes has not been changed measurably by the Starfish explosion. Measurements on Explorer XV (1962 B-λ1) and Telstar I before and after the USSR explosions on October 28 and November 1 show no measurable change in the energetic proton flux (References 27 and 36).

THE SOVIET HIGH ALTITUDE EXPLOSIONS

On October 27, 1962, NASA launched the Explorer XV satellite to study the artificial radiation belt. But before it got in the air there were two artificial belts, and by the time it was up for a day there was a third belt. The Soviets conducted high altitude explosions on October 22 and 28 and then a third one on November 1. Explorer XV had electron detectors on it to cover the range of energies expected for fission electrons, detectors with thresholds from 1/2 Mev to 5 Mev. Figure 11 shows the distribution of electrons for two of Brown's threshold detectors† on Explorer XV. Curves A and C were taken just after Explorer XV was launched, and curves B and D were about 5 hours later after the second Soviet explosion. The new belt of electrons from the explosion is clearly evident, starting at $L = 1.8$ and extending out to about $L = 3$. The inner edge of the new belt is quite sharp, perhaps indicating expansion of the debris from the explosion preferentially upwards as in a field free bubble. Inside about $L = 1.7$ the electron fluxes were essentially unchanged by the Soviet explosions. The little bump on curve A of Figure 11 at $L \approx 1.8$ is probably residue from the Soviet explosion of October 22; this explosion was detected also by Telstar I (Reference 27).

The polar-orbiting Air Force satellite 1962 βK carried several radiation detection instruments to study the artificial belts. The five-channel magnetic electron spectrometer (Reference 31) on

*Filz, R., Yagoda, H., and Holeman, E., "Observations on Trapped Protons in Emulsions Recovered from Satellite Orbits," paper delivered at COSPAR meeting, Warsaw, June 1963. (Proceedings to be published.)
†Private communication from W. L. Brown and J. D. Gabbe.

this vehicle measured electrons of energies 0.3 to 3.2 Mev. This instrument detected the October 28 Soviet explosion and found that at about L = 1.9 the electrons had roughly a fission spectrum but at higher L values the spectrum became softer. It would appear from this that the explosion site was at about L = 1.8 and the higher L electrons were softened maybe in the same way that the Starfish electrons were. The Explorer XV detectors also indicate that the energy spectrum of the electrons introduced by the Soviet October 28 explosion became softer with increasing L.*

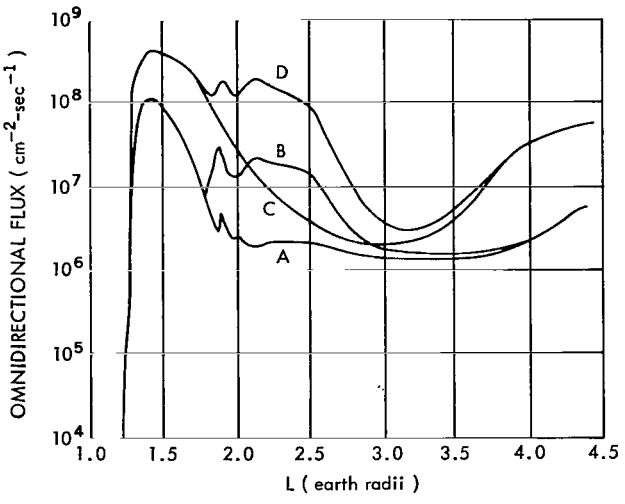

Figure 11—Distribution of electrons along the equator before and after the Soviet October 28 high altitude explosion for two different threshold detectors on Explorer XV: (A) E > 1.9 Mev Oct. 28 at ≈ 0400 UT; (B) E > 1.9 Mev Oct. 28 at ≈ 0900 UT; (C) E > 0.5 Mev Oct. 28 at ≈ 0400 UT; (D) E > 0.5 Mev Oct. 28 at ≈ 0900 UT (from Brown and Gabbe).

Several directional detectors on 1962 βK showed that the electrons injected on October 28 had a flux distribution appropriate to a source well off the equator (Reference 37). This is what we would expect for an explosion at a few hundred kilometers altitude. Detectors on 1962 βK measured the time history of the artificial belt of October 28 and then detected the injection of new electrons in a rather limited new belt at about L = 1.8 on November 1. In both cases the flux of the new particles decreased with time constants of a few days, and the low energy particles seemed to disappear faster (Reference 37).

About a week after the Soviet explosions, the particles injected at L > 1.7 had decayed some. The spatial distribution of E > 5 Mev electrons measured on November 10 by McIlwain (Reference 36) on Explorer XV is shown in Figure 12. The remains of the Starfish belt below L = 1.7 are clearly present as well as the Soviet artificial belt at L = 1.8. The E > 5 Mev flux existing out to L = 4 is probably due mostly to the Soviet explosions, with perhaps some left over from Starfish. Since there are not thought to be any E > 5 Mev electrons in the natural Van Allen belt, Figure 12 is probably made up of electrons from the several explosions.

CHANGES OF THE ELECTRON ENERGY SPECTRUM WITH L

From the Soviet explosion of October 28 the electron spectrum is a fission spectrum for L = 1.8, but the energy spectrum gets consistently softer with increasing L (Reference 31). Why does the energy spectrum change with altitude? It might be due to a combination of two different sources of particles with different spatial distributions, but this seems unlikely. We have no good

*See footnote, page 18, re Brown and Gabbe.

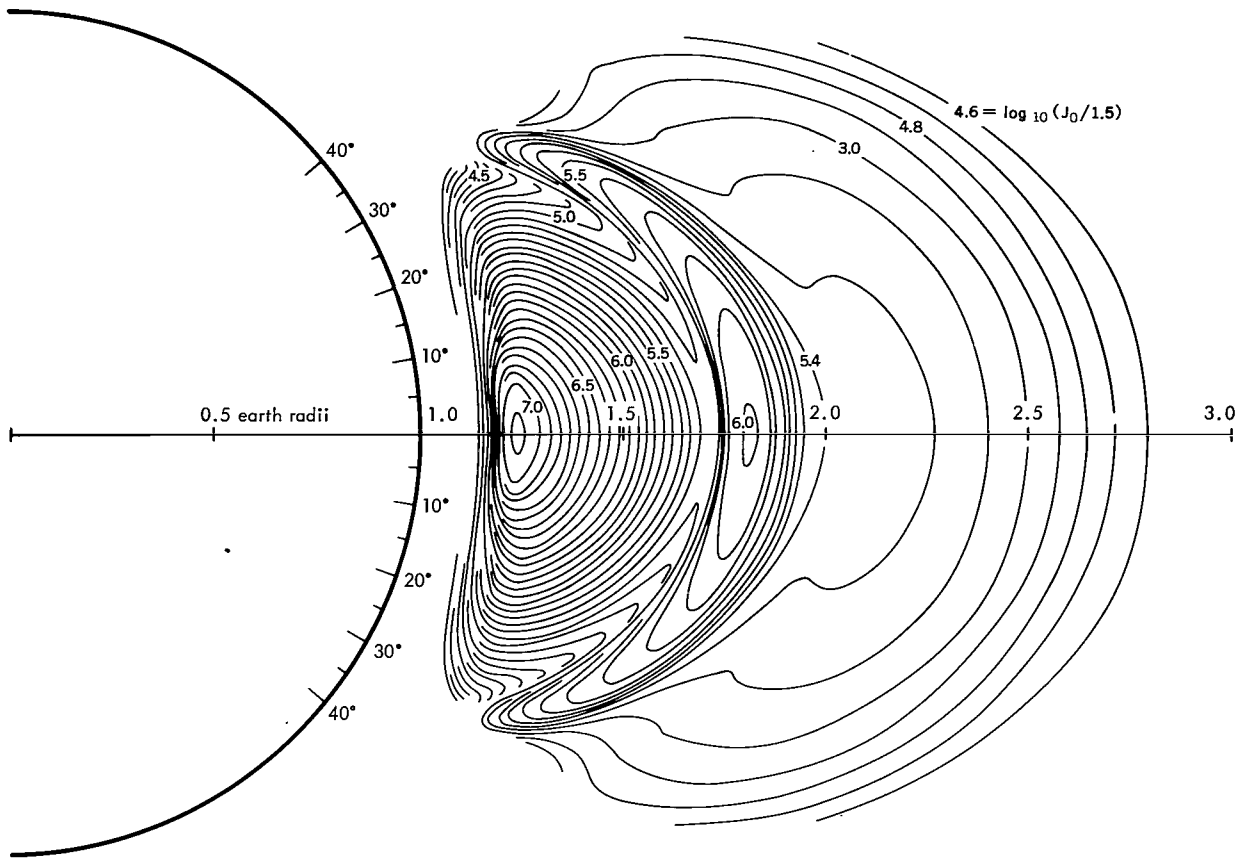

Figure 12—Distribution of E > 5 Mev electrons in R-λ space on November 10 from Explorer XV (from Reference 36).

idea what the second electron source would be. There are two other reasons why the electrons from fission decay might have different energies at different locations.

1. Time after Fission:

The equilibrium fission energy spectrum shown in Figure 8, curve A, is the electron spectrum from a reactor, but this is actually a composite of a variety of energy spectra at different times after the fission event. High energy electrons are given off earlier after fission. Figure 13 shows how the energy spectrum changes with time after fission (Reference 38). From the experimental data on the Soviet October 28 explosion it would appear necessary to have fission fragments remain in space for several hours in order to get the required spectral softening at L = 1.57. This seems like a very long time, but it is not impossible. Colgate (Reference 4) has suggested that most of the fission fragments from the explosion may be slowed down by the expanding debris picking up air. In this way the fission fragments may become slow enough so that the β-spectrum will change some, but we consider it unlikely that they will stay aloft for an hour.

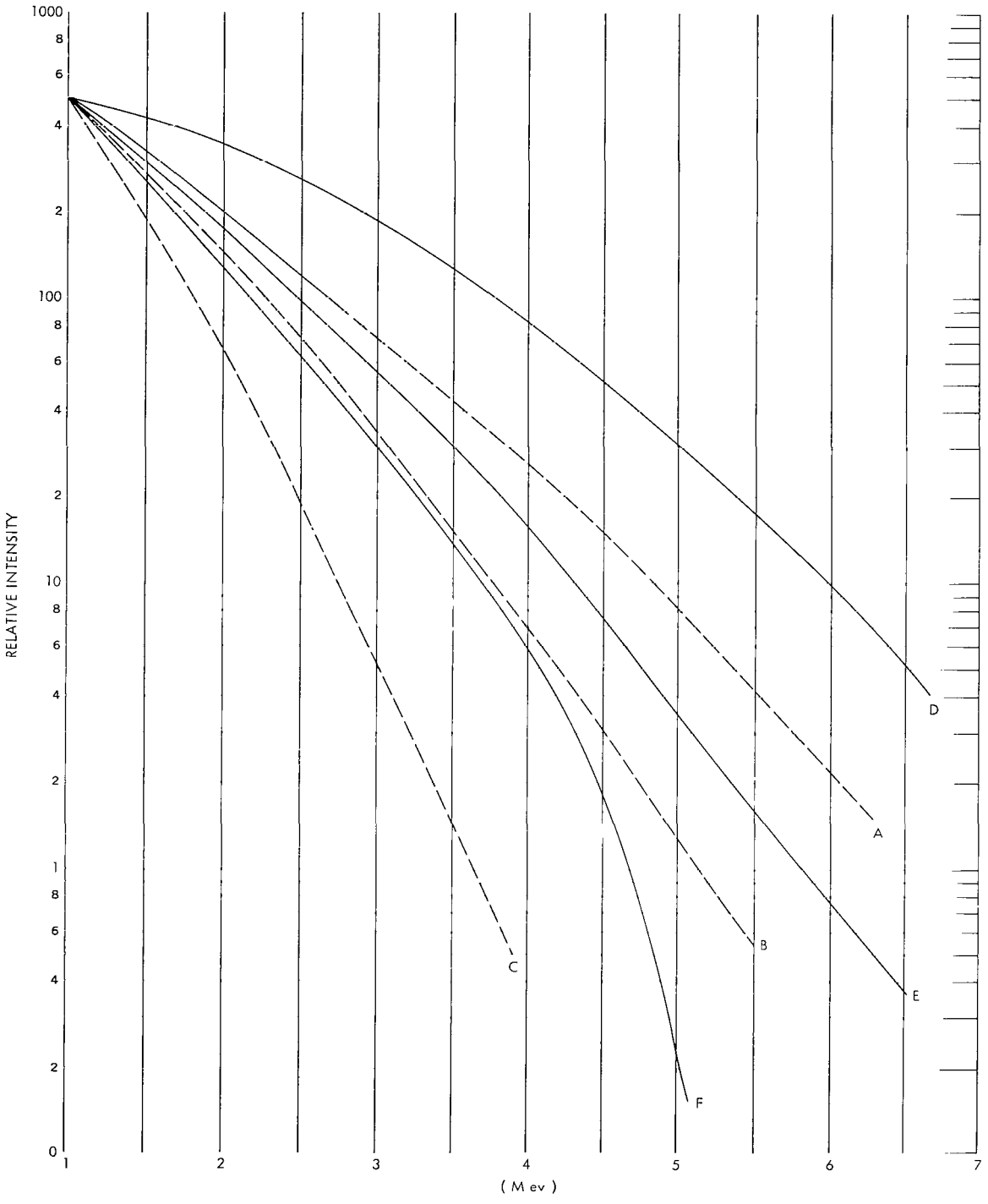

Figure 13–Various electron energy spectra: (A) the equilibrium fission energy spectrum; (B) the fission spectrum softened by a bubble expansion of $l/l_0 = 4/3$; (C) the fission spectrum softened by a bubble expansion of $l/l_0 = 2$; (D) the fission energy spectrum 1 second after fission; (E) the fission energy spectrum 5 minutes after fission; (F) the fission energy spectrum 2.4 hours after fission.

2. Particle Cooling in an Expanding Bubble:

If the electrons are confined in a bubble in the magnetic field and if the bubble expands, the particles will lose energy by colliding with the receding wall.

We can calculate the slowing down of the fast electrons in an expanding bubble as a form of Fermi acceleration (Reference 39).* Starting with a particle of energy E in the bubble, we can study the reflection of the particle at the bubble wall by Lorentz transforming to the system in which the wall is at rest (denoted by E', p'):

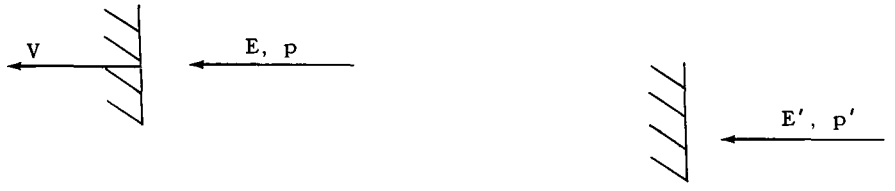

$$p' = \gamma p - \beta\gamma E ,$$
$$E' = \beta\gamma p + \gamma E .$$

The reflection from the stationary wall keeps the energy constant and reverses the momentum. Now, transforming back to the laboratory,

$$E'' = -\beta\gamma p'c + \gamma E' = -\beta\gamma(\gamma pc - \beta\gamma E) + \gamma(-\beta\gamma pc + \gamma E)$$
$$= -2\beta\gamma^2 pc + \gamma^2(1 + \beta^2)E$$
$$= -2\beta\gamma^2\beta^* E + \gamma^2(1 + \beta^2)E ,$$

where $\beta^* c$ is the velocity of the electron, βc is the wall velocity, and $pc = \beta^* E$. The fractional energy loss per collision is

$$f = \frac{E'' - E}{E} = -2\beta\gamma^2\beta^* + \gamma^2(1 + \beta^2) - 1 .$$

For $\beta << 1$, expanding gives

$$f = -2\beta\beta^* + 0(\beta^2) .$$

*D. Hamlin of Convair Astronautics and others have made calculations similar to this.

For fission electron $\gamma^* \approx 1$, so

$$f \approx -2\beta .$$

The number of collisions a particle has per second with the wall is

$$n = \frac{c}{\ell} ,$$

where ℓ is the bubble diameter. The rate of energy loss of a particle is

$$\frac{dE}{dt} = Efn = \frac{-2\beta Ec}{\ell} , \quad \frac{dE}{E} = \frac{-d\ell}{\ell} ;$$

which integrates to

$$\frac{E}{E_0} = \frac{\ell_0}{\ell} ,$$

where E_0 and ℓ_0 are the initial particle energy and bubble radius.

Now, considering a distribution of energies,

$$N(E_0)\, dE_0 = N(E)\, dE \left(\frac{dE_0}{dE}\right)$$

$$= \frac{\ell}{\ell_0} N\left(\frac{\ell_0}{\ell} E_0\right) dE .$$

This expression, which shows how an initial energy spectrum will change as the bubble expands, is plotted in Figure 13 for an initial fission energy spectrum. From this we see that for a bubble expansion ratio $\ell/\ell_0 = 2$, the spectrum will soften enough to match the observations at $L = 1.57$.

For the Soviet explosion of October 28 conducted roughly at $L = 1.8$, to produce electrons on the $L = 3.0$ line a bubble would have to expand at least 1600 km sideways or more in other directions. During the bubble expansion of a factor of 2 starting from ℓ_0 of several hundred kilometers, the trapped particles will hit the bubble walls about 10^3 times. What fraction of the electrons will escape from the bubble during the expansions? If a particle scatters into the loss cone at the end of the bubble, it will leak out. If the reflections at the wall are like diffuse scattering, the bubble will probably be empty after 1000 collisions with the wall. But for specular reflections some reasonable fraction of the particles should stay in the bubble.

One feature of the electron distribution from the October 28 explosion is interesting. There are clearly two peaks in the flux distribution versus L (Reference 37).* It may be that the lower

*See footnote, p. 18, re Brown and Gabbe.

flux peak at $L = 1.8$ is due to electrons from fission fragments that have been trapped on the field lines close to the explosion and that the other peak is due to electrons released from a bubble that has expanded upwards from the explosion site. If this is the case, it would appear that Fermi deceleration of particles in the bubble is the process responsible for changing the electrons' energies. It would not appear that expansion of neutral fission fragments from the explosion site and subsequent β-decay could explain the double-peaked flux distribution easily.

The observations on the energy spectrum from the USSR October 28 explosion help in understanding the Starfish electron flux. The energy spectrum softens with increasing L for the Soviet explosion. Whatever the explanation of this effect is, it seems reasonable to assume that the same effect will be present for all large high-altitude nuclear explosions. Therefore we expect to find lower energy electrons at large L values in the radiation belt made by Starfish, as we do experimentally.

DECAY OF THE ELECTRONS

One of the most interesting features of the Starfish artificial radiation belt has been its decay. Instruments on several satellites have observed the particle population for several months, and certain general features of the decay have been found. At low altitudes the decay is rapid because of interactions with the atmosphere. At high altitudes the decay is quite fast, too—but for a different reason. The atmosphere clearly is not responsible for this loss. In a region in between these two rapid decay zones, the decay is slow but seems to be controlled by the thin atmosphere at high altitudes.

Before the advent of these explosions the only methods of estimating electron lifetimes were indirect. In dealing with a steady state situation where the particle population is moderately constant with time, the only way to measure the lifetime τ of a trapped particle is by measuring either I, the inflow, or O, the outflow, of particles from the radiation belt and using the "leaking bucket" equation

$$I = O = \frac{Q}{\tau} ,$$

or some similar procedure. Here Q is the total number of particles trapped in the volume of the belt association with the inflow I, or outflow O. In the past, the values obtained this way have involved estimates of the outflow O down into the atmosphere and have produced widely different values of τ. We now have direct measurements of τ from the decay of the artificial radiation belts which eliminate the necessity of using this indirect method, which is suspect anyway.

In discussing the decay of the Starfish electrons, it is appropriate to split the problem into two parts: one for high altitude, and one for low altitude.

L < 1.7

In this region of space there is a rapid initial decay at low altitudes, followed by a slow decay afterwards due to coulomb scattering with atmospheric atoms. Van Allen, Frank, and O'Brien measured the decay of the artificial electrons at 1000 km with the Injun satellites;* this is shown in Figure 14. After the initial rapid decay, which is larger for large B values (or low altitude), the decay slows down and is nearly constant for all B values. Measurements on Alouette (1962 B-α1) from September 1962 to January 1963 of the decay of the Starfish electrons (Reference 30) gave time constants of several months for the region $1.3 < L < 1.6$. McIlwain studied the trapped Starfish electrons on Explorer XV for about 3 months, starting in October 1962. He found that, for $1.25 < L < 1.7$, the decay constants were typically greater than 1 year and in some cases are more than 3 years (Reference 36).

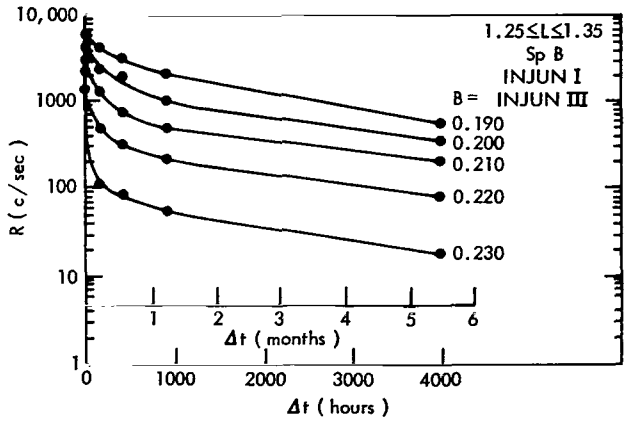

Figure 14—Decay of the Starfish electron flux for low L values measured by the Injun satellites (from Van Allen, Frank, and O'Brien).

At lower altitudes the decay is faster. Glass† has measured the electron decay at 400 km and has found that the decay for several months after Starfish could be described by the law

$$\phi(t) = \frac{\phi(0)}{1 + t/20} ,$$

where t is the time in days.

The decay of trapped electrons controlled by the atmosphere can be calculated in a straightforward way. MacDonald and Walt (Reference 40) have derived a Fokker-Planck equation that describes how a distribution of electrons in space and energy will change with time as the result of coulomb scattering. This has been used by Welch, Kaufmann, and Hess (Reference 41) to study electron time histories.

Neglecting cross field diffusion and neglecting large angle scattering, the time change of a distribution of electrons U in space and energy is obtained by using the Fokker-Planck equation,

$$\frac{\partial U}{\partial t} = -\frac{\partial}{\partial B}\left[< \delta B > U\right] - \frac{\partial}{\partial \gamma}\left[< \delta \gamma > U\right] + \frac{1}{2}\frac{\partial^2}{\partial B^2}\left[< (\delta B)^2 > U\right] .$$

*Van Allen, J. A., Frank, L. A., and O'Brien, B. J., 1963, to be published.
†Gaines, E. E., and Glass, R. A., 1963, to be published.

The distribution function U is defined as the number of particles at time t in a magnetic flux tube of flux dF, mirroring in the magnetic field interval dB at B, and having energies in $d\gamma$ at γ, where γ is the relativistic dimensionless energy

$$\gamma = \frac{E}{m_0 c^2} .$$

The terms in the < > above are the time rates of change of the quantities involved which result from atmospheric coulomb scattering. The atmospheric model used in the calculation is that of Harris and Priester (Reference 42) near solar minimum. The atmosphere is averaged over local time and is also averaged over longitude, considering that a particle's mirror point changes altitude as the particle drifts in longitude. The < > terms are evaluated using small angle coulomb scattering. A tube of force is broken up into 100 space cells of equal ΔB, and the fission energy spectrum used was broken up into nine regions of $\Delta\gamma$ of about 0.75 Mev each. For a starting condition U was taken to be constant all along a field line. Then the problem was run on a computer to watch the distribution change in time.

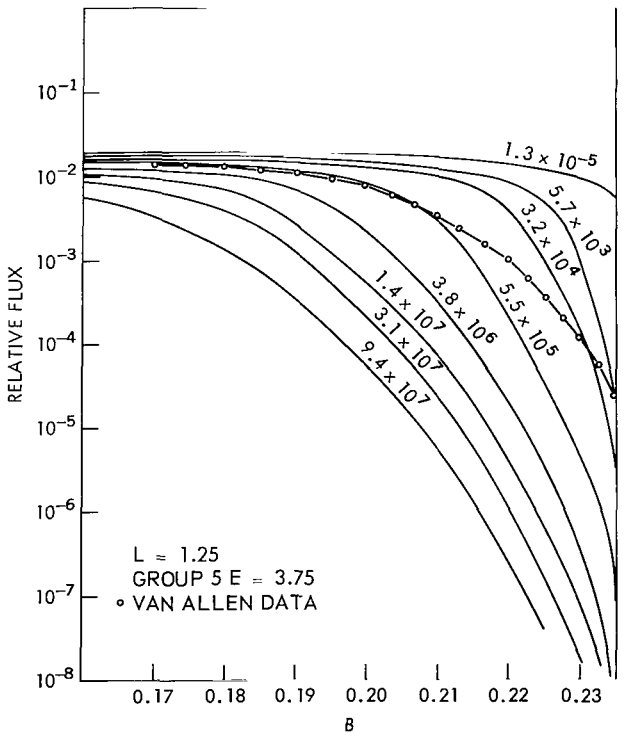

Figure 15—Calculated time histories of 3.75 Mev electrons for L = 1.25. Each curve is labeled by the time after injection in seconds. The data used for comparison show a smooth line drawn through the data in Reference 25 and are for about 1 week after Starfish (from Reference 41).

The results of such a calculation are shown in Figure 15. The electrons at large B (or low altitude) are lost first and, as time progresses, the particles nearer the equator are lost. Eventually an equilibrium develops where scattering up the tube of force is balanced by scattering down the tube, so that the spatial distribution stays constant and the whole distribution then decays in time maintaining its shape. For this equilibrium the decay rate is controlled by the rate of scattering at the equator and is therefore slow compared with the initial decay at low altitudes. The comparison with the experimental data from Injun in Figure 15 shows that the calculation removes particles at large B faster than it should. Recent changes in the Harris and Priester model atmosphere increasing the He density should make the agreement better. The decay rates given by the calculation agree reasonably well with the experimental data. The variation of decay constants with altitude and also the change of τ with time (as indicated

by the changes from Alouette τ's to McIlwain's τ's in the same region but at different times) is in agreement with theoretical expectations.

The decay for early times can be expressed approximately as

$$\phi(B, t) = \phi(B, 0) \frac{\tau}{t + \tau},$$

where $\tau(B)$ is a characteristic decay time. This decay law gradually merges into an exponential decay as scattering equilibrium is reached.

The decay represented in Figure 15 is what is expected for the atmosphere near solar minimum and will probably be reasonably good for the next year or so. But, as solar activity picks up and we get close to solar maximum, the decay will increase very markedly. A large fraction of the Starfish electrons still trapped now will be lost before solar maximum.

During the process of atmospheric scattering, the electron energy spectrum changes. The lower energy electrons are more easily scattered and are therefore lost first. Because of this, the fission energy spectrum hardens with time until an equilibrium spectrum is developed with a peak at about 2 Mev. The Fokker-Planck calculations show this process developing as in Figure 16.

The spectrometer (Reference 31) flown on 1962 βK measured an electron energy spectrum at $L = 1.25$ (see Figure 8, curve B) in December 1962 which is quite similar to the calculated hardened fission spectrum in Figure 16, curve G. From a comparison of the several detectors aloft (Reference 24) at early times after Starfish, the spectrum seemed fission-like down to 1/2 Mev to $L = 1.25$. Therefore the lack of low energy particles in the $L = 1.25$ spectrum in December is not due to an initial paucity but rather to a loss of them after they were trapped. This is what is expected from coulomb scattering.

An electron spectrometer (Reference 34) flown on another Air Force satellite in September 1962 measured an energy spectrum quite similar to curve B in Figure 8 for $1.2 < L < 1.6$; this confirmed the existence of a hardened fission spectrum.

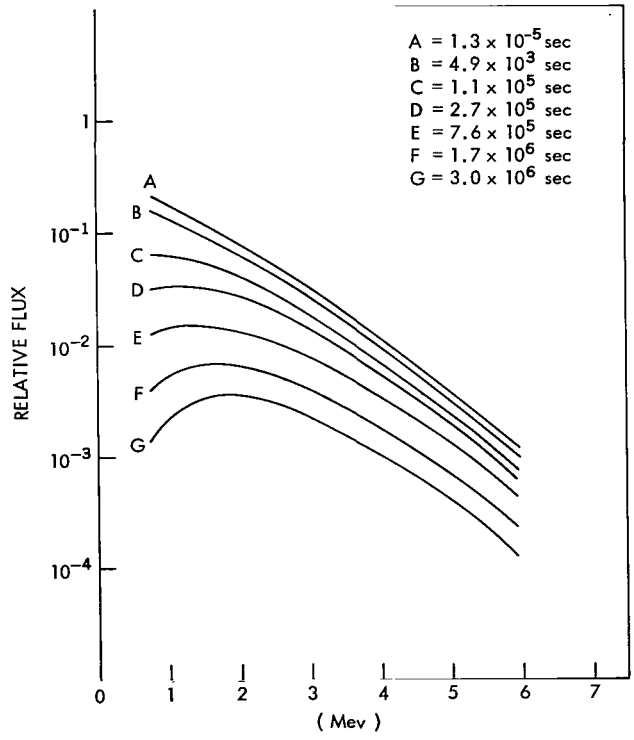

Figure 16—Change in the fission electron energy spectrum with time resulting from coulomb scattering for L = 1.18 and B = 0.20 (from Reference 41).

L > 1.7

The situation is quite different for $L > 1.7$. Brown and Gabbe measured on Telstar I (Reference 27) the decay of the transient electron population introduced into space by the Starfish explosion. They found the decay curves in Figure 17 for $L > 1.7$. In this region of space the electron population decays with short time constants. At $L = 1.7$ the decay constant is many months but, by $L = 2.2$, $\tau \approx 1$ week. It seems impossible for this rapid decay to be due to the atmosphere. It is very likely due to some kind of magnetic disturbances which breaks down one of the adiabatic invariants. Although there are several ideas about the types of disturbances involved (References 43, 44), the real nature of this process is not known.

Measurements made after the three USSR explosions for $L > 1.7$ give decay constants quite similar to the earlier Telstar data. McIlwain (Reference 36) on Explorer XV found the decay was quite steady and monotonic for $L \approx 3$ after November 1. But, for $L \approx 4$, the decay is quite different. There are several stepwise decreases in the flux apparently related to magnetic storms.

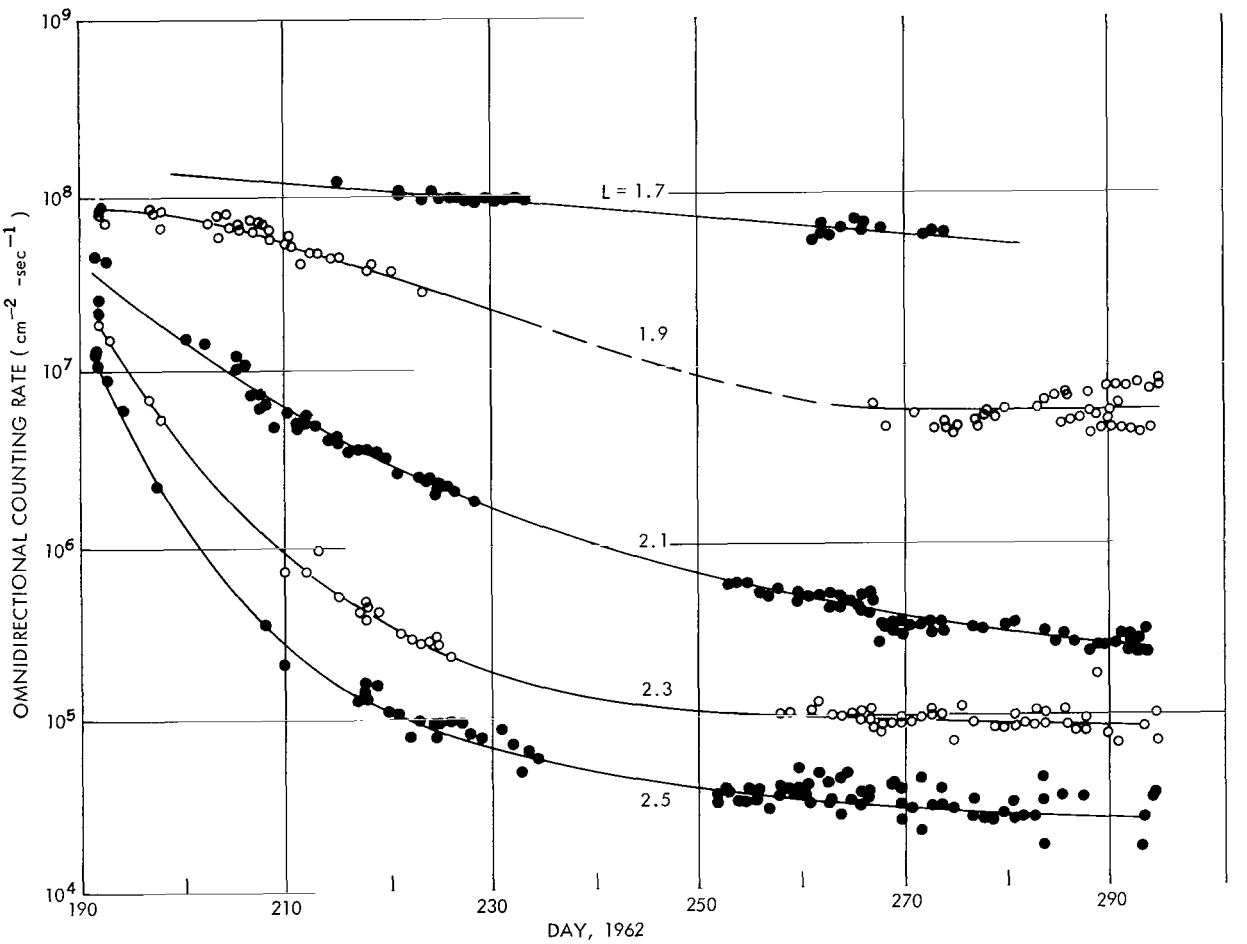

Figure 17—Time decay of the Starfish electron flux for $L > 1.7$ measured on Telstar I (from Reference 27).

On December 18 a large increase in the electron flux occurred at the time of a new magnetic storm. The increase of the $E = 5$ Mev electrons at this time was more than a factor of 10 and made the flux roughly what it was shortly after the USSR explosions. This increase looks suspiciously like particle acceleration. Electrons of $E = 5$ Mev are not thought to exist in the natural belt, so it would appear that this change on December 18 was due to acceleration of particles already there rather than to injection of new particles.

Measurements on Telstar I (Reference 27) after the USSR explosions also show the rapid decay of these new electrons for $L > 1.7$. By studying the time decay of the Starfish electrons, we have learned a considerable amount about the natural radiation belt. We know that electrons in the inner zone of the natural Van Allen belt have long lifetimes and that those in the outer zone have short lifetimes. This information would have been very difficult, if not impossible, to obtain by observing only the steady state natural radiation belt. This is a very important contribution to our understanding of the radiation belts.

What we have learned from Starfish shows that much can be accomplished by carrying out controlled charged particle-injection experiments in space by nuclear explosions. Similar studies could be carried out in the future by using radioactive isotopes or small particle accelerators. Experiments are possible on the production of artificial auroras, artificial VLF disturbances, artificial ionospheric disturbances, and related upper atmospheric chemical processes. Also, more work is needed in trapped particle lifetimes, acceleration and loss processes. This should be an important field of future experimentation.

(Manuscript received August 23, 1963)

REFERENCES

1. Christofilos, N. C., "The Argus Experiment," *J. Geophys. Res.* 64(8):869-875, August 1959.
2. Van Allen, J. A., McIlwain, C. E., and Ludwig, G. H., "Satellite Observations of Electrons Artifically Injected into the Geomagnetic Field," *J. Geophys. Res.* 64(8):877-891, August 1959.
3. Glasstone, S., ed., "The Effects of Nuclear Weapons," Washington, D. C.: U. S. Atomic Energy Commission, 1957.
4. Colgate, S. A., "The Phenomenology of the Mass Motion of a High Altitude Nuclear Explosion," Lawrence Radiation Laboratory Report, UCLRL 7224.
5. Kileen, J., Hess, W. N., and Lingenfelter, R. E., "Electrons from Bomb Neutron Decay," *J. Geophys. Res.* 68(16):4637-4644, August 15, 1963.
6. Zmuda, A. J., Shaw, B. W., and Haave, C. R., "Very Low Frequency Disturbances and the High-Altitude Nuclear Explosion of July 9, 1962," *J. Geophys. Res.* 68(3):745-768, February 1, 1963.
7. Allcock, G. McK., Branigan, C. K., Mountjoy, J. C., and Helliwell, R. A., "Whistler and Other Very Low Frequency Phenomena Associated with the High-Altitude Nuclear Explosion on July 9, 1962," *J. Geophys. Res.* 68(3):735-740, February 1, 1963.

8. Wilson, C. R., and Sugiura, M., "Hydromagnetic Waves Generated by the July 9, 1962, Nuclear Weapons Test as Observed at College, Alaska," *J. Geophys. Res.* 68(10):3149-3154, May 15, 1963.

9. Crook, G. M., Greenstadt, E. W., and Inouye, G. T., "Distant Electromagnetic Observations of the High-Altitude Nuclear Detonation of July 9, 1962," *J. Geophys. Res.* 68(6):1781-1784, March 15, 1963.

10. Gregory, J. B., "New Zealand Observations of the High-Altitude Explosion of July 9 at Johnston Island," *Nature*, 196(4854):508-511, November 10, 1962.

11. Basler, R. P., Dyce, R. B., and Leinbach, H., "High-Latitude Ionization Associated with the July 9 Explosion," *J. Geophys. Res.* 68(3):741-744, February 1, 1963.

12. Armstrong, R. J., and Wharton, A. E. B., "Effects of the High-Altitude Thermonuclear Explosion of July 9, 1962, 0900 UT, Observed at Jamaica," *J. Geophys. Res.* 68(6):1779-1780, March 15, 1963.

13. Rothwell, P., Wager, J. H., and Sayers, J., "Effect of the Johnston Island High-Altitude Nuclear Explosion on the Ionization Density in the Topside Ionosphere," *J. Geophys. Res.* 68(3):947-949, February 1, 1963.

14. Latter, R., and LeLevier, R. E., "Detection of Ionization Effects from Nuclear Explosions in Space," *J. Geophys. Res.* 68(6):1643-1666, March 15, 1963.

15. Ochs, G. R., Farley, D. T., Jr., Bowles, K. L., and Bandyopadhay, P., "Observations of Synchrotron Radio Noise at the Magnetic Equator Following the High-Altitude Nuclear Explosion of July 9, 1962," *J. Geophys. Res.* 68(3):701-711, February 1, 1963.

16. Schwinger, J., "On the Classical Radiation of Accelerated Electrons," *Phys. Rev.* 75:1912-1925, June 15, 1949.

17. Chang, D. B., and Davis, L., Jr., "Synchrotron Radiation as the Source of Jupiter's Polarized Decimeter Radiation," *Astrophys. J.* 136(2):567-581, September 1962.

18. Peterson, A. M., and Hower, G. L., "Synchrotron Radiation from High-Energy Electrons," *J. Geophys. Res.* 68(3):723-734, February 1, 1963.

19. Nakada, M. P., "Synchrotron Radiation Calculations for the Artificial Radiation Belt," *J. Geophys. Res.* 68(13):4079-4090, July 1, 1963.

20. Dyce, R. B., and Horowitz, S., "Measurements of Synchrotron Radiation at Central Pacific Sites," *J. Geophys. Res.* 68(3):713-721, February 1, 1963.

21. Durney, A. C., Elliot, H., Hynds, R. J., and Quenby, J. J., "Satellite Observations of the Energetic Particle Flux Produced by the High-Altitude Nuclear Explosion of July 9, 1962," *Nature*, 195(4848):1245-1247, September 29, 1962.

22. Pieper, G. F., Williams, D. J., and Frank, L. A., "Traac Observations of the Artificial Radiation Belt from the July 9, 1962, Nuclear Detonation," *J. Geophys. Res.* 68(3):635-640, February 1, 1963.

23. Pieper, G. F., "A Second Radiation Belt from the July 9, 1962, Nuclear Detonation," *J. Geophys. Res.* 68(3):651-656, February 1, 1963.

24. Hess, W. N., "The Artificial Radiation Belt Made on July 9, 1962," *J. Geophys. Res.* 68(3):667-683, February 1, 1963.

25. O'Brien, B. J., Laughlin, C. D., and Van Allen, J. A., "Geomagnetically Trapped Radiation Produced by a High-Altitude Nuclear Explosion on July 9, 1962," *Nature* 195(4845):939-942, September 8, 1962.

26. Brown, W. L., and Gabbe, J. D., "The Electron Distribution in the Earth's Radiation Belts During July 1962 as Measured by Telstar," *J. Geophys. Res.* 68(3):607-618, February 1962.

27. Brown, W. L., Gabbe, J. D., and Rosenzweig, W., "Results of the *Telstar* Radiation Experiments," *Bell System Tech. J.* 42(4-3):1505-1560, July 1963.

28. Van Allen, J. A., Frank, L. A., and O'Brien, B. J., "Satellite Observations of the Artificial Radiation Belt of July 1962," *J. Geophys. Res.* 68(3):619-627, February 1, 1963.

29. Kellogg, P. J., Ney, E., and Winckler, J., "Geophysical Effects Associated with High Altitude Explosions," *Nature* 183:358, 1958.

30. McDiarmid, I. B., Burrows, J. R., Budzinski, E. E., and Rose, D. C., "Satellite Measurements in the Starfish Artificial Radiation Zone," *Con. J. Phys.* 41:1332, 1963.

31. West, H. I., Mann, L. G., and Bloom, S. D., "Spectra and Fluxes of Electrons Trapped in the Earth's Magnetic Field Followed Recent High Altitude Nuclear Bursts," AFCRL Report, Interim Results of Radiation Measurements from Air Force Satellite 1962 βK, June 17, 1963.

32. Smith, R. V., and Imhof, W. L., "Satellite Measurements of the Artificial Radiation Belt," *J. Geophys. Res.* 68(3):629-634, February 1, 1963.

33. Rosenzweig, W., Gummel, H. K., and Smits, F. M., "Solar Cell Degradation Under 1-Mev Electron Bombardment," *Bell System Tech. J.* 42(2):399-414, March 1963.

34. Mozer, F. S., Elliott, D. D., Mihalov, J. D., Paulikas, G. A., Vampola, A. L., and Freden, S. C., "Preliminary Analysis of the Fluxes and Spectrums of Trapped Particles after the Nuclear Test of July 9, 1962," *J. Geophys. Res.* 68(3):641-650, February 1, 1963.

35. Fischell, R. E., "Solar Cell Performance in the Artificial Radiation Belt," *AIAA Jour.* 1(1):242-245, January 1963.

36. McIlwain, C. E., "The Radiation Belts, Natural and Artificial," *Science* 142:355, 1963.

37. Katz, L., Smart, D., Paolini, F. R., Giacconi, R., and Talbot, R. J., "Measurements on Trapped Particles Injected by Nuclear Detonations," AFCRL Report Interim Results of Radiation Measurements from Air Force Satellite 1962 βK, June 17, 1963.

38. West, H. I., Lawrence Radiation Laboratory Report UCRL 6123 T, 1960.

39. Fermi, E., "On the Origin of Cosmic Radiation," *Phys. Rev.* 75(8):1169-1174, April 15, 1949.

40. MacDonald, W. M., and Walt, M., "Distribution Function of Magnetically Confined Electrons in a Scattering Atmosphere," *Ann. Phys.* 15(1):44-62, July 1961.

41. Welch, J. A., Jr., Kaufmann, L., and Hess, W. N., "Trapped Electron Time Histories for L = 1.18 to L = 1.30," *J. Geophys. Res.* 68(3):685-700, February 1, 1963.

42. Harris, I., and Priester, W., "Theoretical Models for the Solar-Cycle Variation of the Upper Atmosphere," NASA Technical Note D-1444, 1962.

43. Parker, E. N., "Effect of Hydromagnetic Waves in a Dipole Field on the Longitudinal Invariant," *J. Geophys. Res.* 66(3):693-708, March 1961.

44. Dungey, J. W., "Resonant Effect of Plasma Waves on Charged Particles in a Magnetic Field," *J. Fluid Mech.* 15:74-82, January 1963.

2/7/85

"The aeronautical and space activities of the United States shall be conducted so as to contribute . . . to the expansion of human knowledge of phenomena in the atmosphere and space. The Administration shall provide for the widest practicable and appropriate dissemination of information concerning its activities and the results thereof."

—NATIONAL AERONAUTICS AND SPACE ACT OF 1958

NASA SCIENTIFIC AND TECHNICAL PUBLICATIONS

TECHNICAL REPORTS: Scientific and technical information considered important, complete, and a lasting contribution to existing knowledge.

TECHNICAL NOTES: Information less broad in scope but nevertheless of importance as a contribution to existing knowledge.

TECHNICAL MEMORANDUMS: Information receiving limited distribution because of preliminary data, security classification, or other reasons.

CONTRACTOR REPORTS: Technical information generated in connection with a NASA contract or grant and released under NASA auspices.

TECHNICAL TRANSLATIONS: Information published in a foreign language considered to merit NASA distribution in English.

TECHNICAL REPRINTS: Information derived from NASA activities and initially published in the form of journal articles.

SPECIAL PUBLICATIONS: Information derived from or of value to NASA activities but not necessarily reporting the results of individual NASA-programmed scientific efforts. Publications include conference proceedings, monographs, data compilations, handbooks, sourcebooks, and special bibliographies.

Details on the availability of these publications may be obtained from:

SCIENTIFIC AND TECHNICAL INFORMATION DIVISION

NATIONAL AERONAUTICS AND SPACE ADMINISTRATION

Washington, D.C. 20546